

Novel Isothermal Amplification Integrated with CRISPR/Cas13a and Its Applications for Ultrasensitive Detection of SARS-CoV-2

Jaemin Kim, Yo Rim Kim, Sang Mo Lee, Jinhwan Lee, Seoyoung Lee, Dongeun Yong,* and Hyun Gyu Park*



Cite This: <https://doi.org/10.1021/acssynbio.4c00605>



Read Online

ACCESS |

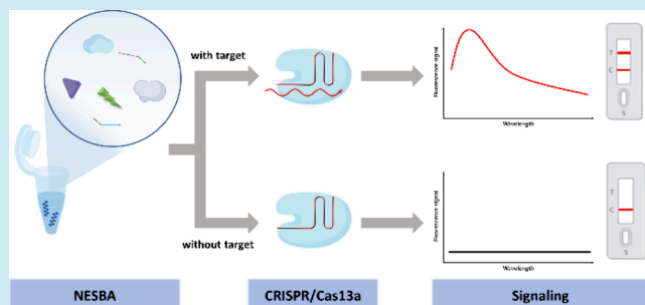
Metrics & More

Article Recommendations

Supporting Information

ABSTRACT: We herein developed an ultrasensitive and rapid strategy to identify genomic nucleic acids by integrating a clustered regularly interspaced short palindromic repeats (CRISPR)/CRISPR-associated protein 13a (Cas13a) into our recently developed isothermal technique, nicking and extension chain reaction system-based amplification (NESBA) reaction. In this technique, named CESBA, the NESBA reaction isothermally produces a large amount of RNA amplicons from the initial target genomic RNA (gRNA). The RNA amplicons bind to the crisper RNA (crRNA) and activate the collateral cleavage activity of Cas13a, which would then cleave the reporter probe nearby, consequently producing the final signals. Based on this design principle, we successfully detected SARS-CoV-2 gRNA as a model target very sensitively down to even a single copy (0.05 copies/ μ L) in both fluorescence- and lateral flow assay (LFA)-based modes with excellent specificity against other human coronaviruses (H-CoVs). We further validated the clinical applicability of CESBA by testing the 20 clinical samples with 100% clinical sensitivity and specificity. This work represents a potent and innovative strategy for the identification of genomic nucleic acids in molecular diagnostics, delivering exceptional levels of sensitivity.

KEYWORDS: isothermal amplification, NESBA, CRISPR/Cas13a, lateral flow assay, COVID-19, SARS-CoV-2



Throughout human history, the detection and identification of infectious pathogens, including viruses and bacteria, have played a pivotal role in public health and medicine.^{1–3} The ability to rapidly and accurately identify these microorganisms has been instrumental in controlling epidemics and pandemics, preventing the spread of diseases, and saving countless lives.^{4,5} The recent COVID-19 pandemic has highlighted the critical importance of molecular diagnostics in the battle against infectious diseases, underscoring the need for innovative and efficient techniques to identify the nucleic acids of the pathogens.^{6,7}

Quantitative polymerase chain reaction (qPCR) is the current gold standard for nucleic acid detection, providing high clinical sensitivity and specificity.^{8–10} However, qPCR requires a thermal cycler to precisely control the temperature, skilled personnel, and centralized clinics or laboratories, which might limit its widespread applications for point-of-care testing (POCT) in resource-limited settings.^{11–14} As alternatives, isothermal amplification methods have been developed, including strand displacement amplification (SDA),¹⁵ loop-mediated isothermal amplification (LAMP),¹⁶ rolling circle amplification (RCA),¹⁷ recombinase polymerase amplification (RPA),¹⁸ nucleic acid sequence-based amplification (NASBA),¹⁹ nicking enzyme amplification reaction

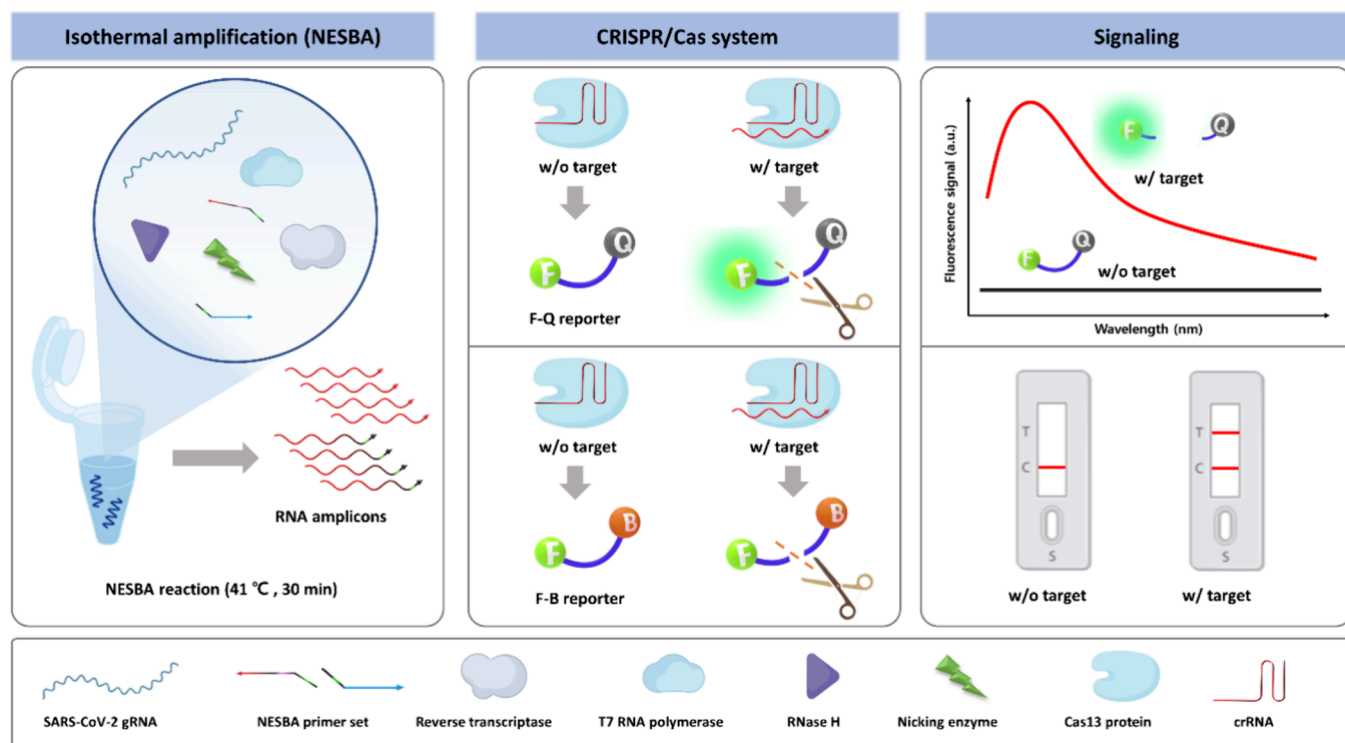
(NEAR),²⁰ and so on.^{21–23} They have advantages such as being easy to miniaturize and having a relatively rapid reaction time by eliminating a thermal cycler and denaturation step. However, they also possess several limitations, such as poor sensitivity, nonspecific amplification, and the complicated reaction procedure.^{24–26}

Meanwhile, the clustered regularly interspaced short palindromic repeat (CRISPR)/CRISPR-associated protein (Cas) technique has been effectively integrated into isothermal amplification to enhance sensitivity and specificity.²⁷ Representative, Cas12a and Cas13a have been applied to detect target nucleic acids utilizing their collateral cleavage activity.^{28,29} Among them, the trans-cleavage activity of Cas13a is activated through the recognition for the crRNA-complementary RNA sequence, which would cleave nearby single-stranded RNA with superior activity over Cas12a.³⁰ Since Cas13a is activated by single-stranded RNA targets, an additional transcription step is

Received: September 3, 2024

Revised: January 13, 2025

Accepted: January 14, 2025

Scheme 1. Overall Procedure to Identify Genomic Nucleic Acids by CESBA.^a

^aThe arrow indicates the 3' end of the nucleic acid strand

required to integrate the Cas13a system into the existing very powerful isothermal amplification methods such as RPA and LAMP.^{31,32}

Upon this background, we integrated the Cas13a system into our recent isothermal technique, nicking and extension chain reaction system-based amplification (NESBA) system,^{33,34} capable of producing a large amount of RNA amplicons from the initial target gRNA, and developed a new CRISPR/Cas13a-based NESBA (CESBA) technique for detecting target nucleic acids. In this technique, Cas13a was activated by recognizing RNA amplicons produced by the NESBA reaction, and the triggered collateral cleavage activity of Cas13a cleaved the RNA reporter, which could produce the signals to identify target nucleic acids. With the proposed strategy, we successfully identified SARS-CoV-2 gRNA, yielding excellent sensitivity and specificity in both fluorescence- and LFA-based modes.

METHODS

Materials. All DNA oligonucleotides employed in this study were synthesized and purified with PAGE by Bioneer (Daejeon, Korea). RNA oligonucleotides were synthesized and HPLC-purified by Integrated DNA Technology, Inc. (IDT, Coralville, IA, USA). All DNA and RNA sequences are listed in Table S1. LwCas13a and 10X Cas13a Buffer (50 mM MgCl₂, 1 mM EDTA, 1 M NaCl, and 200 mM HEPES) were purchased from MCLAB (San Francisco, USA). NASBA enzyme cocktail and 3X NASBA buffer (36 mM MgCl₂, 210 mM KCl, pH 8.5, 30 mM DTT, 120 mM Tris-HCl, and 45% DMSO) were purchased from Life Science Advanced Technologies Inc. (St Petersburg, FL, USA). Nt. alwI, rNTPs, dNTPs, and 10X NEBuffer 2.1 (100 mM MgCl₂, 1 mg/mL BSA, 100 mM Tris-HCl, 500 mM NaCl, pH 7.9, and) were purchased from New England Biolabs Inc. (Beverly, MA, USA). The gRNAs of HCoV-NL63, MERS-CoV,

and SARS-CoV-2 (BetaCoV/Korea/KCDC03/2020) were supplied by the National Culture Collection for Pathogens (Cheongju, Korea). The gRNAs of HCoV-OC43 and HCoV-229E were purchased from the Korea Bank for Pathogenic Viruses (Seoul, Korea), and SARS-CoV and HCoV-HKU-1 were purchased from IDT. The HybriDetect Universal Lateral Flow Assay Kit was purchased from Milenia Biotec (Versailler Str. 1, Giessen, Germany). Nuclease-free water was purchased from Bioneer and used in all the experiments.

The CESBA Reaction for SARS-CoV-2 Detection. Twenty μ L of the reaction solution were prepared by mixing 1 μ L of 10X NEBuffer 2.1, 6.7 μ L of 3X NASBA buffer, 1.4 μ L of primer set (20 μ M each), 1.4 μ L of dNTPs (10 mM each), 2.8 μ L of rNTPs (25 mM each), 0.2 μ L of DW, 0.5 μ L of Nt.AlwI (10 U/ μ L), 5 μ L of NASBA enzyme cocktail (4X), and 1 μ L of an analyte containing target nucleic acid. The solution was incubated at 41 °C for 30 min.

Two μ L of the NESBA reaction solution and 0.8 μ L RNA reporter were added to the Cas13a reaction solution containing 2 μ L of Cas13a (1 μ M), 2 μ L of 10X Cas13a buffer, 2 μ L of crRNA (1 μ M), and 11.2 μ L of DW, which was preincubated at 37 °C for 15 min. Next, the solution mixture was incubated at 37 °C for 10 min and then subjected to the final detection step. In a fluorescence-based mode, we used an RNA reporter labeled with FAM and quencher (F-Q reporter), and measured the fluorescent signals from 500 to 600 nm with excitation wavelength of 460 nm using 384-well Greiner Bio-One microplates (ref. 781077, Courtaboeuf, France) and a Tecan Infinite M200 pro microplate reader (Männedorf, Switzerland). In an LFA-based mode, an RNA reporter labeled with FAM and biotin (F-B reporter) was used. The conjugation pad of the HybriDetect dipstick was dipped into a mixture of the Cas13a reaction solution and HybriDetect assay buffer for 1.5 min. The

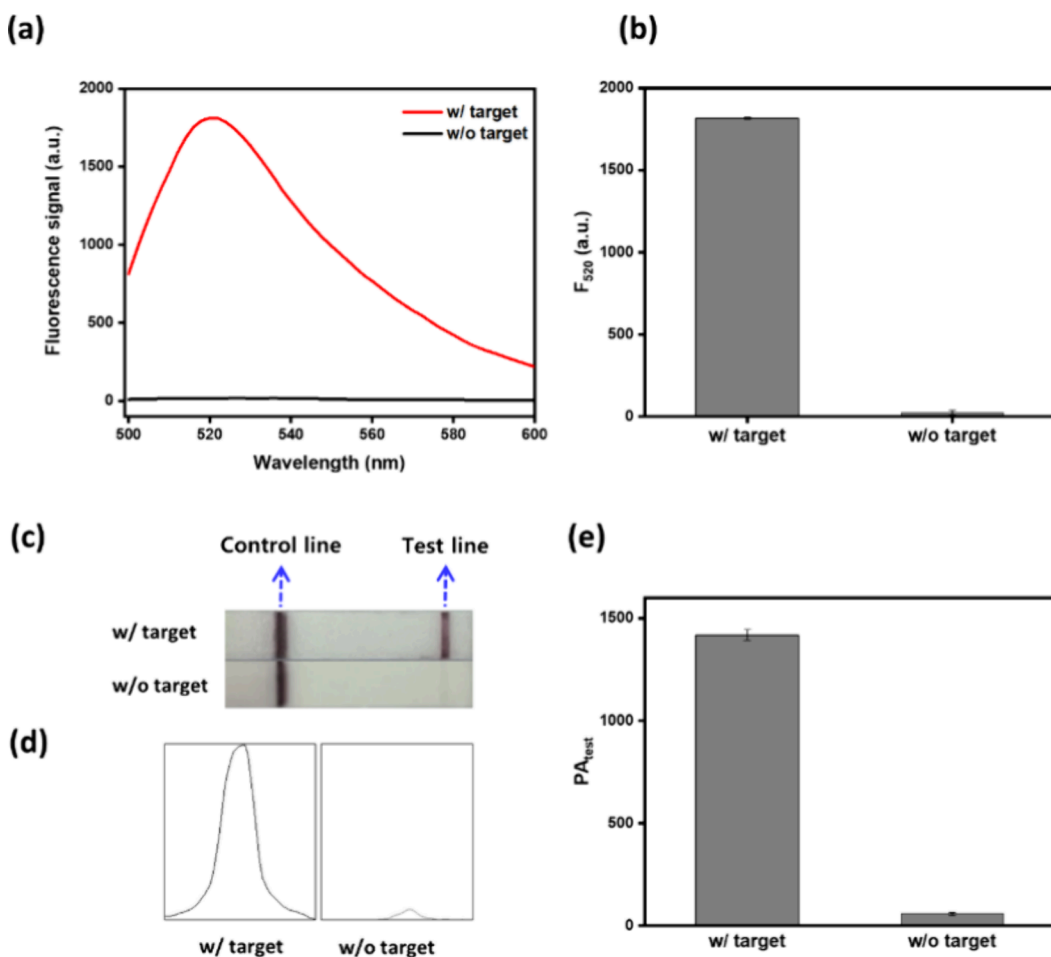


Figure 1. CESBA reaction for nucleic acid detection. (a) Fluorescence emission spectra, (b) the fluorescence intensity at 520 nm (F_{520}), (c) photographic image of the LFA dipsticks, (d) band intensity graph of the test line, and (e) peak areas of the test line (PA_{test}) obtained from the samples with and without target gRNA. The final concentrations of target gRNA, F-Q reporter, and F-B reporter are 10^7 copies/reaction, 200 nM, and 500 nM, respectively. Error bars were estimated from triplicate tests.

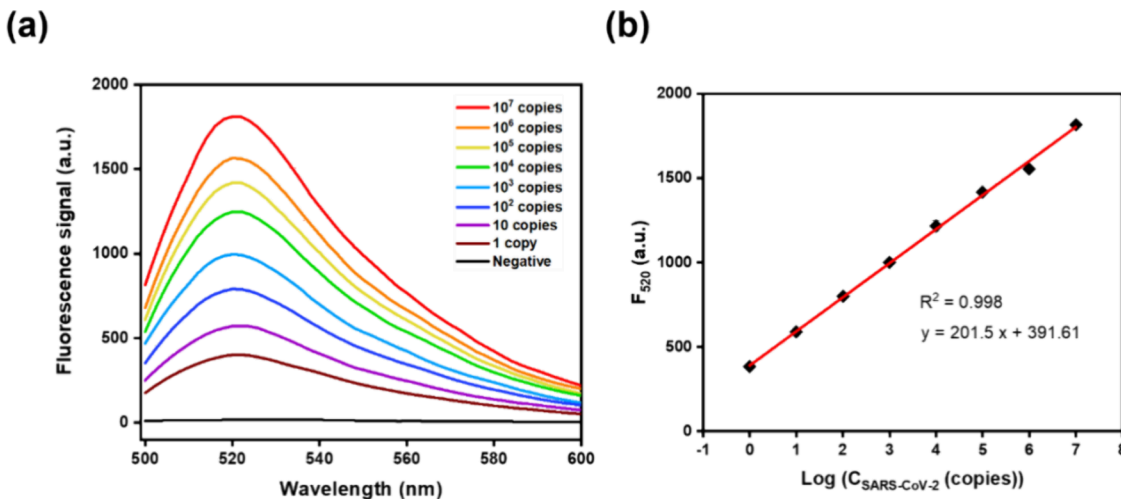


Figure 2. Sensitivity of the fluorescence-based CESBA reaction. (a) Fluorescence emission spectra of the reaction products with SARS-CoV-2 gRNA at various concentrations in the range from 1 copy to 10^7 copies/reaction. (b) The linear relationship between fluorescence intensity at 520 nm (F_{520}) and the logarithmic concentration of SARS-CoV-2 gRNA ($C_{SARS-CoV-2}$). Error bars were estimated from triplicate tests.

peak area of the test line was measured using ImageJ (National Institutes of Health, Bethesda, MD, USA).

In the clinical applicability test, a total of 20 clinical samples were collected from individuals suspected of having SARS-CoV-

2 infection and placed in universal transport medium. This study was approved and reviewed by Severance hospital (IRB approval number: 4-2020-0465; Seoul, Korea). The AdvanSure Nucleic Acid R kit (LG chem, Seoul, Korea) was used to extract the

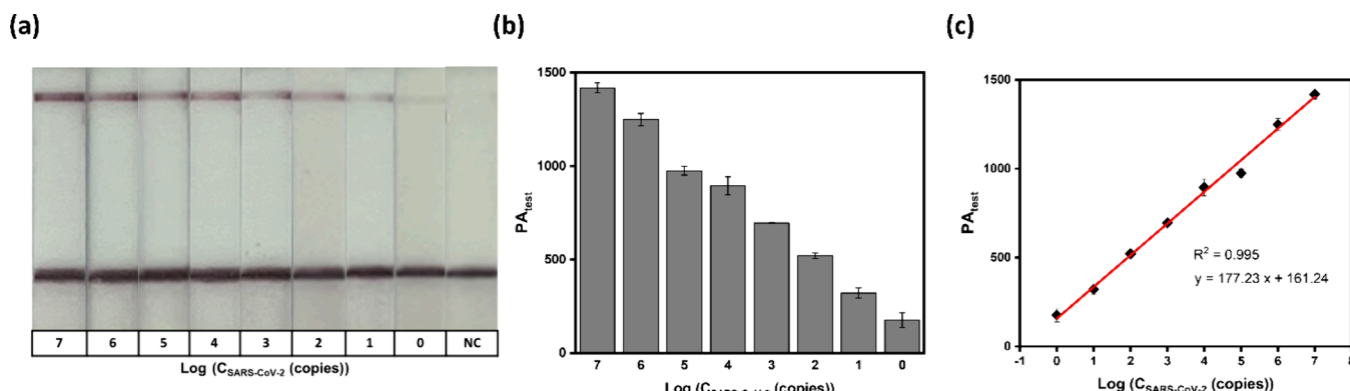


Figure 3. Sensitivity of the LFA-based CESBA reaction. (a) Photographic image of the LFA dipsticks with SARS-CoV-2 gRNA at various concentrations in the range from 1 copy to 10^7 copies/reaction. (b) Peak areas of the test line (PA_{test}). (c) The linear relationship between the PA_{test} and the logarithmic $C_{SARS-CoV-2}$. Error bars were estimated from triplicate tests.

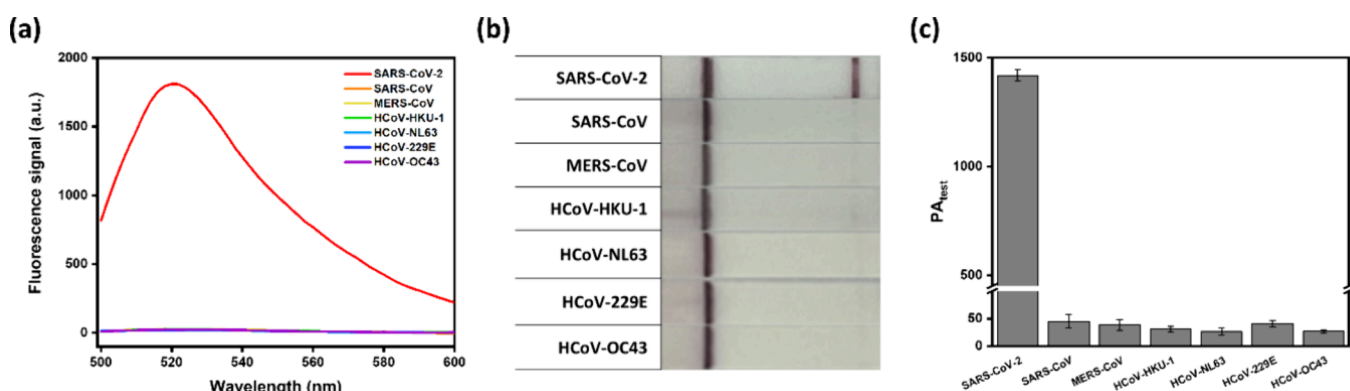


Figure 4. Specificity of the fluorescence- and LFA-based CESBA reaction. (a) Fluorescence emission spectra, (b) photographic image of the LFA dipsticks, and (c) peak areas of the test line (PA_{test}) obtained from the reaction products with SARS-CoV-2 gRNA and other types of HCoV such as SARS-CoV, MERS-CoV, HCoV-HKU-1, HCoV-229E, HCoV-NL63, and HCoV-OC43. The final concentrations of SARS-CoV-2 gRNA, other viral RNAs for all seven HCoVs, F-Q reporter, and F-B reporter are 10^7 copies/reaction, 10^7 copies/reaction, 200 nM, and 500 nM, respectively. Error bars were estimated from triplicate tests.

gRNAs from the clinical samples, and the gRNAs were subjected to CESBA as described above.

Clinical Sample Testing with qRT-PCR. The same clinical samples were also analyzed by the qRT-PCR method with the Allplex 2019-nCoV assay kit (Seegene, Seoul, Korea). They were reverse transcribed for 20 min at 50°C , followed by initial denaturation for 15 min at 95°C . PCR was then performed with 45 cycles of 15 s at 94°C and 30 s at 58°C with the fluorescent signal being measured every cycle using the CFX96 Real-Time System (Bio-Rad).

RESULTS AND DISCUSSION

Overall Principle of the CESBA Reaction. As depicted in Scheme 1, this strategy consists primarily of three steps: (i) isothermal amplification of RNA amplicons through the NESBA reaction; (ii) recognition of RNA amplicons by CRISPR/Cas13a and reporter probe cutting by the activated Cas13a's collateral cleavage activity; and (iii) signaling by fluorescence or LFA.

The NESBA reaction is an advanced version of nucleic acid sequence-based amplification (NASBA) that employs a primer set designed to contain an additional nicking enzyme recognition site. Briefly, the presence of target gRNA leads to the formation of T7 promoter-containing double-stranded DNA (T7DNA) and produces a large number of RNA amplicons via the following transcription-mediated amplification (Figure S1).

In this work, the RNA amplicons produced through the NESBA reaction complementarily bind to the crRNA in the crRNA/Cas13a complex and trigger the collateral cleavage activity of Cas13a, which consequently cleaves the employed RNA reporter. The FAM and quencher-labeled reporter (F-Q reporter) and the FAM and biotin-labeled reporter (F-B reporter) are used in the fluorescence-based and LFA-based modes, respectively.

The LFA dipstick is composed of the conjugation pad, the control line, and the test line in order, where the control line and the test line have a biotin ligand (streptavidin) and antirabbit antibodies, respectively. When the conjugation pad of the dipstick is dipped in the LFA solution, FAM on the 5' end of the reporter binds to the gold-labeled anti-FAM antibody (Au-FAM Ab) that is present on the conjugation pad. In the absence of target gRNA, the intact reporter/Au-FAM Ab complexes bind to the biotin ligand via the reporter's 3' end biotin, resulting in a red-colored band on the control line. There is no red-colored band on the test line since the experimental settings were designed so that the control line could accommodate all of the complexes and none could reach it. On the other hand, the presence of target gRNA cleaves the reporters, producing the cleaved reporter fragments having only 5' end FAM or 3' end biotin. The cleaved reporters with FAM are complexed with Au-FAM Ab, which would bind to the antirabbit antibodies on the test line, making a red-colored band. The experimental

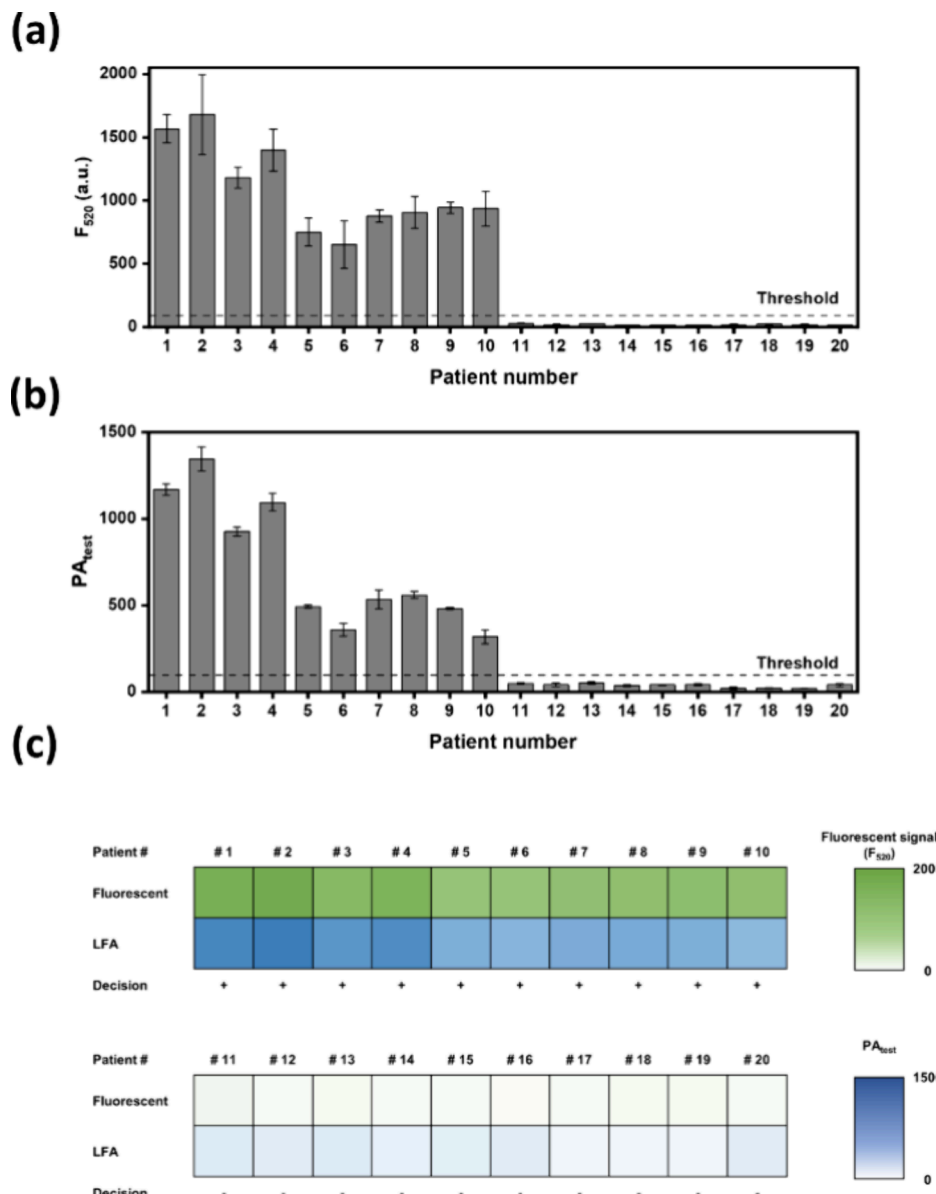


Figure 5. Diagnosis of COVID-19 using the CESBA reaction. (a) The fluorescence intensity at 520 nm (F_{520}) and (b) the peak area of the test line (PA_{test}) obtained from the reaction solution for clinical samples. The final diagnosis decision was determined based on diagnostic thresholds (background +5SD) and error bars indicate the standard deviation of triplicate tests. (c) Heatmap of the F_{520} and the PA_{test} values obtained from the reaction products.

conditions were set up so that not all of the reporters were completely cleaved and that some uncleaved ones were trapped by biotin ligands, resulting in a red band on the control line as well.

Analytical Performance of the CESBA Reaction. To maximize the CESBA reaction efficiency, we optimized several reaction conditions by examining the fluorescence intensity at 520 nm (F_{520}) obtained from the CESBA reaction solution in the presence and absence of target gRNA. As described in Figure S2–S3, 200 nM of crRNA/Cas13a and 10 min of Cas13 reaction time were selected as the optimal conditions. We also optimized F–B reporter concentration by measuring the peak area of the test line (PA_{test}) obtained from the dipstick in the absence and presence of target gRNA. As presented in Figure S4, 500 nM of F–B reporter was selected as the optimal concentration. Under the optimized conditions, we successfully discriminated the target gRNA in the two modes by producing the enhanced

fluorescence signal and the intense test line band in the presence of target gRNA (Figure 1).

Next, we examined the fluorescence emission spectra and F_{520} acquired from the CESBA reactions for the samples containing target gRNA at different concentrations in the range of 1 copy to 10^7 copies. As shown in Figure 2(a), the fluorescence signal exhibited a positive correlation with concentrations of SARS-CoV-2 ($C_{SARS-CoV-2}$). When the F_{520} was plotted against the logarithm of the $C_{SARS-CoV-2}$, it showed an excellent linear relationship ($F_{520} = 201.5 \log(C_{SARS-CoV-2}) + 391.61$, $R^2 = 0.998$) (Figure 2(b)). Remarkably, the limit of detection was determined to be a single copy (0.05 copies/ μ L), offering much superior levels of sensitivity over the previous alternative techniques (Table S2).

To determine the sensitivity of the LFA-based mode, we also tested the same sample solutions in the same range and produced the final signals on the LFA strips. We acquired the

photographic images and measured the intensity of the red-colored band on the test line, which showed a positive correlation between the PA_{test} and the $C_{SARS-CoV-2}$ (Figure 3(a), (b)). When the PA_{test} was plotted against the logarithm of $C_{SARS-CoV-2}$, an excellent linear relationship ($PA_{test} = 177.23 \log(C_{SARS-CoV-2}) + 161.24$, $R^2 = 0.995$) was obtained (Figure 3(c)). As evidenced in Figure 3(a), even a single copy of SARS-CoV-2 gRNA was clearly identified in the LFA-based mode, which has never been achieved before (Table S2).

Specificity of the CESBA reaction was assessed by employing various human coronaviruses (HCoVs), including HCoV-HKU-1, HCoV-NL63, HCoV-229E, HCoV-OC43, SARS-CoV, and MERS-CoV. As shown in Figure 4, the highly enhanced fluorescence signal and clear red-colored band on the test line were observed only in the presence of SARS-CoV-2 gRNA, whereas negligible fluorescence enhancement and band on the test line were detected from the other HCoVs. These results clearly demonstrated the excellent specificity of the CESBA reaction.

Clinical Applicability of the CESBA Reaction. The clinical applicability of the CESBA reaction was demonstrated by testing 20 clinical specimens in the two modes based on the threshold values defined as the background signal plus five times the standard deviation of the blank. As illustrated in Figure 5(a), the fluorescence-based CESBA approach assessed ten samples as positive and ten samples as negative. The LFA-based CESBA approach tested the identical samples equally positive or negative (Figure 5(b)). In order to visually compare the diagnosis outcomes, we also displayed a heatmap based on the F_{520} and PA_{test} (Figure 5(c)). It should be noted that the fluorescence-based mode appears to be more discriminating between positive and negative samples. We also performed qRT-PCR on the same samples to validate the results, and the results were completely consistent with the CESBA reaction (Table S3-4). All of these findings indicate that the CESBA reaction can be practically used to test clinical specimens with 100% clinical sensitivity and specificity.

CONCLUSIONS

In this work, we developed an ultrasensitive and specific technique to identify nucleic acids, named CESBA. The CESBA reaction principally relies on our own isothermal NESBA technique, integrated into the CRISPR/Cas13a system. Based on this developed method, we successfully identified SARS-CoV-2 gRNA down to even a single copy (0.05 copies/ μ L) in both the fluorescence- and LFA-based modes with excellent specificity very rapidly within 40 min. Very importantly, this is the first report to achieve single-copy identification by LFA-based methods. By delivering unparalleled sensitivity, the developed CESBA system assumes a pivotal role in the timely detection and effective control of infectious diseases, promising to be a cornerstone in the field of diagnosis.

ASSOCIATED CONTENT

Supporting Information

The Supporting Information is available free of charge at <https://pubs.acs.org/doi/10.1021/acssynbio.4c00605>.

Oligonucleotide sequences (Table S1); schematic illustration of NESBA (Figure S1); optimization of various reaction conditions (Figures S2–S4); comparison of the proposed method with previous COVID-19 testing

(Table S2); clinical testings by qRT-PCR and CESBA (Table S3) (PDF)

AUTHOR INFORMATION

Corresponding Authors

Dongeun Yong – Department of Laboratory Medicine and Research Institute of Bacterial Resistance, Yonsei University College of Medicine, Seoul 03722, Republic of Korea; Email: deyong@yuhs.ac

Hyun Gyu Park – Department of Chemical and Biomolecular Engineering (BK21 Four), Korea Advanced Institute of Science and Technology (KAIST), Daejeon 34141, Republic of Korea; orcid.org/0000-0001-9978-3890; Email: hgpark@kaist.ac.kr

Authors

Jaemin Kim – Department of Chemical and Biomolecular Engineering (BK21 Four), Korea Advanced Institute of Science and Technology (KAIST), Daejeon 34141, Republic of Korea

Yo Rim Kim – Department of Chemical and Biomolecular Engineering (BK21 Four), Korea Advanced Institute of Science and Technology (KAIST), Daejeon 34141, Republic of Korea

Sang Mo Lee – Department of Chemical and Biomolecular Engineering (BK21 Four), Korea Advanced Institute of Science and Technology (KAIST), Daejeon 34141, Republic of Korea

Jinhwan Lee – Department of Chemical and Biomolecular Engineering (BK21 Four), Korea Advanced Institute of Science and Technology (KAIST), Daejeon 34141, Republic of Korea

Seoyoung Lee – Department of Chemical and Biomolecular Engineering (BK21 Four), Korea Advanced Institute of Science and Technology (KAIST), Daejeon 34141, Republic of Korea

Complete contact information is available at:
<https://pubs.acs.org/10.1021/acssynbio.4c00605>

Author Contributions

The manuscript was written through contributions of all authors. All authors have given approval to the final version of the manuscript. Jaemin Kim: conceptualization, methodology, formal analysis, validation, investigation, writing (original draft), visualization; Yo Rim Kim: investigation, formal analysis, writing (original draft); Sang Mo Lee: methodology; Jinhwan Lee: methodology; Jinhwan Lee: methodology; Seoyoung Lee: methodology, investigation; Dongeun Yong: resource; Hyun Gyu Park: visualization, supervision, project administration, funding acquisition.

Notes

The authors declare no competing financial interest.

ACKNOWLEDGMENTS

This research was supported by the Midcareer Researcher Support Program (NRF-2021R1A2B5B03001739) of the National Research Foundation (NRF). Financial support for this work was also provided by the Korea government (MSIT) (2022K1A4A8A01080317 and RS-2023-00218543).

REFERENCES

- (1) França, R.; Da Silva, C.; De Paula, S. O. Recent advances in molecular medicine techniques for the diagnosis, prevention, and control of infectious diseases. *Eur. J. Clin. Microbiol. Infect. Dis.* **2013**, *32*, 723–728.
- (2) Fauci, A. S.; Morens, D. M. The perpetual challenge of infectious diseases. *N. Engl. J. Med.* **2012**, *366* (5), 454–461.

(3) Yager, P.; Domingo, G. J.; Gerdes, J. Point-of-care diagnostics for global health. *Annu. Rev. Biomed. Eng.* **2008**, *10*, 107–144.

(4) Cheon, J.; Qin, J.; Lee, L. P.; Lee, H. Advances in biosensor technologies for infection diagnostics. *Acc. Chem. Res.* **2022**, *55*, 121–122.

(5) Mabey, D.; Peeling, R. W.; Ustianowski, A.; Perkins, M. D. Diagnostics for the developing world. *Nat. Rev. Microbiol.* **2004**, *2* (3), 231–240.

(6) Gao, Z.; Xu, Y.; Sun, C.; Wang, X.; Guo, Y.; Qiu, S.; Ma, K. A systematic review of asymptomatic infections with COVID-19. *J. Microbiol. Immunol. Infect.* **2021**, *S4* (1), 12–16.

(7) Nishiura, H.; Kobayashi, T.; Miyama, T.; Suzuki, A.; Jung, S. M.; Hayashi, K.; Kinoshita, R.; Yang, Y.; Yuan, B.; Akhmetzhanov, A. R.; Linton, N. M. Estimation of the asymptomatic ratio of novel coronavirus infections (COVID-19). *Int. J. Infect. Dis.* **2020**, *94*, 154–155.

(8) Guo, Y.-R.; Cao, Q.-D.; Hong, Z.-S.; Tan, Y.-Y.; Chen, S.-D.; Jin, H.-J.; Tan, K.-S.; Wang, D.-Y.; Yan, Y. The origin, transmission and clinical therapies on coronavirus disease 2019 (COVID-19) outbreak—an update on the status. *Mil. Med. Res.* **2020**, *7* (1), 1–10.

(9) Lu, X.; Wang, L.; Sakthivel, S. K.; Whitaker, B.; Murray, J.; Kamili, S.; Lynch, B.; Malapati, L.; Burke, S. A.; Harcourt, J.; Tamin, A.; Thornburg, N. J.; Villanueva, J. M.; Lindstrom, S. US CDC real-time reverse transcription PCR panel for detection of severe acute respiratory syndrome coronavirus 2. *Emerging Infect. Dis.* **2020**, *26* (8), 1654.

(10) Tahamtan, A.; Ardebili, A. Real-time RT-PCR in COVID-19 detection: issues affecting the results. *Expert Rev. Mol. Diagn.* **2020**, *20* (5), 453–454.

(11) Carter, L. J.; Garner, L. V.; Smoot, J. W.; Li, Y.; Zhou, Q.; Saveson, C. J.; Sasso, J. M.; Gregg, A. C.; Soares, D. J.; Beskid, T. R.; Jersey, S. R.; Liu, C. Assay techniques and test development for COVID-19 diagnosis. *ACS Cent. Sci.* **2020**, *6*, 591–605.

(12) Cui, F.; Zhou, H. S. Diagnostic methods and potential portable biosensors for coronavirus disease 2019. *Biosens. Bioelectron.* **2020**, *165*, No. 112349.

(13) Park, G.-S.; Ku, K.; Baek, S.-H.; Kim, S.-J.; Kim, S. I.; Kim, B.-T.; Maeng, J.-S. Development of reverse transcription loop-mediated isothermal amplification assays targeting severe acute respiratory syndrome coronavirus 2 (SARS-CoV-2). *J. Mol. Diagn.* **2020**, *22* (6), 729–735.

(14) Tang, Y. W.; Schmitz, J. E.; Persing, D. H.; Stratton, C. W.; McAdam, A. J. Laboratory diagnosis of COVID-19: current issues and challenges. *J. Clin. Microbiol.* **2020**, *58* (6), No. e00512-20.

(15) Walker, G. T.; Fraiser, M. S.; Schram, J. L.; Little, M. C.; Nadeau, J. G.; Malinowski, D. P. Strand displacement amplification—an isothermal, in vitro DNA amplification technique. *Nucleic Acids Res.* **1992**, *20* (7), 1691–1696.

(16) Notomi, T.; Okayama, H.; Masubuchi, H.; Yonekawa, T.; Watanabe, K.; Amino, N.; Hase, T. Loop-mediated isothermal amplification of DNA. *Nucleic Acids Res.* **2000**, *28* (12), No. e63.

(17) Lizardi, P. M.; Huang, X.; Zhu, Z.; Bray-Ward, P.; Thomas, D. C.; Ward, D. C. Mutation detection and single-molecule counting using isothermal rolling-circle amplification. *Nat. Genet.* **1998**, *19* (3), 225–232.

(18) Piepenburg, O.; Williams, C. H.; Stemple, D. L.; Armes, N. A. DNA detection using recombination proteins. *PLOS Biol.* **2006**, *4* (7), No. e204.

(19) Compton, J. Nucleic acid sequence-based amplification. *Nature* **1991**, *350*, 91–92.

(20) Van Ness, J.; Van Ness, L. K.; Galas, D. J. Isothermal reactions for the amplification of oligonucleotides. *Proc. Natl. Acad. Sci. U.S.A.* **2003**, *100* (8), 4504–4509.

(21) Kim, H. Y.; Song, J.; Park, H. G. Ultrasensitive isothermal method to detect microRNA based on target-induced chain amplification reaction. *Biosens. Bioelectron.* **2021**, *178*, No. 113048.

(22) Lee, S.; Jang, H.; Kim, H. Y.; Park, H. G. Three-way junction-induced isothermal amplification for nucleic acid detection. *Biosens. Bioelectron.* **2020**, *147*, No. 111762.

(23) Song, J. Y.; Jung, Y.; Lee, S.; Park, H. G. Self-priming hairpin-utilized isothermal amplification enabling ultrasensitive nucleic acid detection. *Anal. Chem.* **2020**, *92* (15), 10350–10356.

(24) Huang, X.; Tang, G.; Ismail, N.; Wang, X. Developing RT-LAMP assays for rapid diagnosis of SARS-CoV-2 in saliva. *EBioMedicine* **2022**, *75*, No. 103736.

(25) Ali, Z.; Aman, R.; Mahas, A.; Rao, G. S.; Tehseen, M.; Marsic, T.; Salunke, R.; Subudhi, A. K.; Hala, S. M.; Hamdan, S. M.; Pain, A.; Alofi, F. S.; Alsomali, A.; Hashem, A. M.; Khogeer, A.; Almontashiri, N. A. M.; Abedalthagafi, M.; Hassan, N.; Mahfouz, M. M. iSCAN: An RT-LAMP-coupled CRISPR-Cas12 module for rapid, sensitive detection of SARS-CoV-2. *Virus Res.* **2020**, *288*, No. 198129.

(26) Nagai, K.; Horita, N.; Yamamoto, M.; Tsukahara, T.; Nagakura, H.; Tashiro, K.; Shibata, Y.; Watanabe, H.; Nakashima, K.; Ushio, R.; Ikeda, M.; Narita, A.; Kanai, A.; Sato, T.; Kaneko, T. Diagnostic test accuracy of loop-mediated isothermal amplification assay for *Mycobacterium tuberculosis*: systematic review and meta-analysis. *Sci. Rep.* **2016**, *6* (1), 39090.

(27) Kaur, N.; Toley, B. J. based nucleic acid amplification tests for point-of-care diagnostics. *Analyst* **2018**, *143* (10), 2213–2234.

(28) Chen, J. S.; Ma, E.; Harrington, L. B.; Da Costa, M.; Tian, X.; Palefsky, J. M.; Doudna, J. A. CRISPR-Cas12a target binding unleashes indiscriminate single-stranded DNase activity. *Science* **2018**, *360* (6387), 436–439.

(29) Patchsung, M.; Jantarug, K.; Pattama, A.; Aphicho, K.; Suraritdechachai, S.; Meesawat, P.; Sappakhaw, K.; Leelakorn, N.; Ruenkan, T.; Wongsatit, T.; Athipanyasip, N.; Eiamthong, B.; Lakkanasirorat, B.; Phoodokmai, T.; Niljianskul, N.; Pakotiprapha, D.; Chanarat, S.; Homchan, A.; Tinikul, R.; Kamutira, P.; Phiwkaow, K.; Soithongcharoen, S.; Kantiwiriyawanit, C.; Pongsupasa, V.; Trisrirat, D.; Jaroensuk, J.; Wongnate, T.; Maenpuen, S.; Chaiyen, P.; Kamnerdnakta, S.; Swangsri, J.; Chuthapisith, S.; Sirivatanauksorn, Y.; Chaimayo, C.; Sutthent, R.; Kantakamalakul, W.; Joung, J.; Ladha, A.; Jin, X.; Gootenberg, J. S.; Abudayyeh, O. O.; Zhang, F.; Horthongkham, N.; Uttamapinant, C. Clinical validation of a Cas13-based assay for the detection of SARS-CoV-2 RNA. *Nat. Biomed. Eng.* **2020**, *4* (12), 1140–1149.

(30) Feng, W.; Zhang, H.; Le, X. C. Signal amplification by the trans-cleavage activity of CRISPR-Cas systems: kinetics and performance. *Anal. Chem.* **2023**, *95* (1), 206–217.

(31) Ortiz-Cartagena, C.; Fernández-García, L.; Blasco, L.; Pachos, O.; Bleriot, I.; López, M.; Cantón, R.; Tomás, M.; Perez, D. R. Reverse Transcription-loop-mediated isothermal Amplification-CRISPR-Cas13a technology as a promising diagnostic tool for SARS-CoV-2. *Microbiol. Spectr.* **2022**, *10* (5), No. e0239822.

(32) Kellner, M. J.; Koob, J. G.; Gootenberg, J. S.; Abudayyeh, O. O.; Zhang, F. SHERLOCK: nucleic acid detection with CRISPR nucleases. *Nat. Protoc.* **2019**, *14* (10), 2986–3012.

(33) Ju, Y.; Kim, H. Y.; Ahn, J. K.; Park, H. G. Ultrasensitive version of nucleic acid sequence-based amplification (NASBA) utilizing a nicking and extension chain reaction system. *Nanoscale* **2021**, *13* (24), 10785–10791.

(34) Ju, Y.; Kim, J.; Park, Y.; Lee, C. Y.; Kim, K.; Hong, K. H.; Lee, H.; Yong, D.; Park, H. G. Rapid and accurate clinical testing for COVID-19 by nicking and extension chain reaction system-based amplification (NESBA). *Biosens. Bioelectron.* **2022**, *196*, No. 113689.